Technology in Cancer Research and Treatment
ISSN 1533-0346
Volume 7, Number 3, June 2008
©Adenine Press (2008)

Differentiation of Melanoma from Non-Cancerous Tissue in an Animal Model Using Elastic Light Single-Scattering Spectroscopy

www.tcrt.org

Murat Canpolat, Ph.D.[1,*]
A. Güzide Gökhan, M.D.[2]
M. Akif Çiftçioğlu, M.D.[2]
Nuray Erin, M.D., Ph.D.[3]

[1]Department of Biophysics
[2]Department of Pathology
[3]Department of Internal Medicine
School of Medicine
Akdeniz University
Dumlupınar Bulvarı Antalya, 07059 Turkey

Cutaneous melanoma is the most serious form of skin cancer and is curable only if it is detected early. The most effective treatment for the melanoma is surgical excision of the lesion. Traditionally, wide margins of excision have been used for effective treatment, but are not always desirable due to increased risk of infection and esthetic reasons. Besides, safe surgical margins of the lesion are not always correlated well with the size of the lesions. We have previously developed a system using elastic light single-scattering spectroscopy to differentiate cancerous tissue from non-cancerous tissue and tested it *in vitro*. The goal of this study was, therefore, to determine the effectiveness of this system *ex vivo* by using a mouse model of melanoma. First, a melanoma cell line; B16F10 were injected subcutaneously at right mid flank region of C57BL6 mice (n=5) and allowed to develop for two weeks. Tumors were dissected and spectra were taken on tumor tissue and on normal looking skin tissue that was 10 mm distant from the incision. Since these tumors become markedly necrotic in the middle, spectra of necrotic area was also taken. Slopes of the spectra were positive taken on non-cancerous skin tissues that were later verified by histological examination. On the other hand, it gave negative slopes on melanomas. Increased sizes of the nuclei correlated with the negative slope while smaller nuclei found in non-cancerous tissue gave positive slope. Spectrum taken from necrotic area differed from both cancerous and non-cancerous tissue such that it gave a U-shaped spectrum. These results demonstrate that elastic light single-scattering spectroscopy system can differentiate cancerous tissue from non-cancerous and has potential to be used intraoperatively to determine the surgical margins.

Key words: Melanoma; Non-Invasive; Elastic Light Scattering Spectroscopy; Detection.

Introduction

Cutaneous malignant melanoma is a rare highly aggressive disease that causes approximately 70% of all deaths from skin cancer. In patients whose melanoma has spread to lymph nodes, survival rates decrease markedly despite new treatment modalities (1). Hence, early diagnosis and adequate surgical interventions are crucial. Traditionally, wide margins of excision are used, but over the past decade, margins have become smaller because previous clinical trials suggested that narrower margins are as safe as wide margins (2-4). Overall survival rates are similar for narrow and wide margin excision (5). However, inadequate excision margins increase the risks of local recurrence and in-transit metastases, both associated with high mortality rate (6). On the other hand, unnecessarily wide margins of excision are associated with greater morbidity and increased cost. Hence, it is crucial to determine intra-operatively appoximate tumor margins.

[*]Corresponding Author:
Murat Canpolat, Ph.D.
Email: Canpolat@akdeniz.edu.tr

Several different techniques can detect skin cancer. These include dermoscopy, epiluminescence microscopy, optical coherence tomography, reflectance confocal microscopy, diffuse reflectance spectroscopy, Raman spectroscopy, fluorescence imaging, tetraherz imaging, and electrical impedance computed tomography. A recent review (7) defined each system and summarized succinctly their advantages and disadvantages.

In practice, currently exist intraoperatively techniques are not completely satisfactory and accurate to detect residual tumor cells at surgical margins. Therefore, new techniques need to be developed and applied to scan margins of excised tissue *in situ*.

Several approaches have used methodology based on light scattering to obtain information about tissues. Diffusion of light, for example, can detect cancer in tissue. Signals are affected by both light absorption and scattering leading inconsistent results (8-11). Spectra of singly scattered light beams are, on the other hand is sensitive only to size of scatters and provide information about the size of scatterers (12-15). There are several ways to detect single beam light scattering. Detecting singly-scattered components of back reflected light is strongly related to experimental design or geometry of optical fiber probe. Previously, single scattered components of back reflected light from tissues were obtained by modeling and subtracting the diffuse component from total back reflected light (12), where, singly scattered light components comprised only a small portion of total back-reflected light and produced a high noise-to-signal ratio.

Polarization light scattering spectroscopy is another method to isolate single scattering components of back reflected light from tissue (13). The most convenient way to detect single scattered light beam from a turbid medium is to use a single optical fiber probe to deliver light to and from tissues. Spectra from elastic light single-scattering spectroscopy (ELSSS) taken by a single optical fiber probe using white light can quantify size of scatterer in a tissue phantom (14, 15). Penetration depth of ~90% of single scattered photons originates from < 200 μm in tissue phantoms. The diffuse component of backscattered light is significantly reduced (15). ELSSS offers a new modality to detect cancerous tissues in real-time (14). This system, however, has not been tested previously *ex vivo* to differentiate cancerous tissue under controlled conditions. The present feasibility study, a limited number of mice (n=5) were used to test the systems' efficiency in differentiating between normal and cancerous tissue. A detailed description of the single optical fiber probe system is provided elsewhere (14).

Materials and Methods

System Description

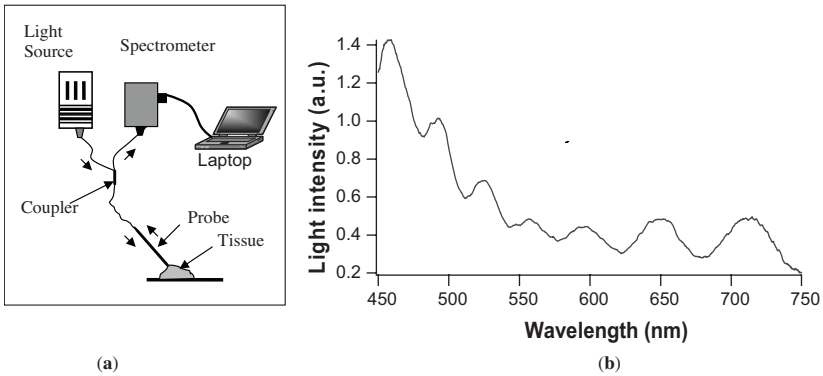
A schematic diagram of ELSSS system appears in Figure 1. The optical system consists of a spectrometer (USB2000, Ocean Optics, Tampa FL), a tungsten halogen white light source, a single optical fiber probe, and a laptop computer. The single optical fiber probe was used for both delivery and detection of white light to and from the tissue, as shown in Figure 1. The single probe was a 1 × 2 fiber optical coupler with splitting ratio of 50%. The proximal end of the coupler was connected to the light source. The distal end was connected to the spectrometer. The diameter of the distal end of the probe's fiber was 100 μm; the numerical apertures was 0.22.

Before initiating experiments, the system was tested by taking ELSSS spectra from a tissue phantom, a mono-dispersed polystyrene microsphere with a 2 μm diameter in water. The measured spectra were corrected for wavelength dependence of system components and specular reflection. The corrected spectrum is provided by the equation:

$$R(\lambda) = \frac{R(\lambda)_s - R(\lambda)_{bg}}{R(\lambda)_c - R(\lambda)_{bg}} \quad [1]$$

where, $R(\lambda)_s$ is a spectrum of the tissue, $R(\lambda)_c$ a spectrum of Spectralon (Labsphere, Inc.) in water and $R(\lambda)_{bg}$ a background spectrum from pure water in a black container.

As shown in Figure 1b, the spectrum of the tissue phantom



(a) (b)

Figure 1: Panel (**a**) demonstrates a single-fiber optical probe system designed to differentiate cancerous from normal tissue. This system consists of a halogen tungsten light source, optical fibers, a coupler, a spectrometer, and a laptop computer. Light travels from the light source to the probe through optical fibers and reflects back from tissue surfaces, finally traveling to spectrometer for analysis. Panel (**b**) shows spectrum from mono sized, 2 μm, polystyrene spheres taken by a single optical fiber probe. Mie oscillations on the spectrum indicate single scattered photons collected by the single fiber optical probe.

has an oscillating pattern, evidence of single Mie scattering from mono-disperse particles (14, 15).

Tumor Model in Mice and Experimental Procedures

Twelve to fifteen week old C57BL/6 mice of both sexes were used in this study. Animals were inbred in Research Animal Facilities Akdeniz University, School of Medicine, Turkey. All protocols were approved by the Animal Research Ethics Committee of Akdeniz University. B16F10 melanoma cells were grown in DMEM-F12 medium supplemented with non-essential amino acids and sodium pyruvate. B16F10 cells (10^6) were injected subcutaneously into the left mid flank region of C57BL/6 mice under ether anesthesia. Two weeks after implantation, tumors reached palpable size (1 cm^3). Prior to spectral analysis, mice were sacrificed using ether.

We performed experiments with *ex vivo* melanoma and adjacent non-cancerous skin tissue samples immediately after surgical resection. The single fiber optical probe gently touched melanoma tissues and normal-looking skin tissue, approximately 10 mm distant from incision areas. Spectra were also taken from macroscopically necrotic areas of the tumor. At least fifteen spectra were obtained at each location. Spectra of disease-free skin distant from tumor inoculation site were used as control. Because B16F10 cells do not metastasize when inoculated subcutaneously, there was no need to sacrifice control animals to obtain cancer-free tissues. Furthermore, to verify the non-cancerous nature of disease-free skin, as well as to determine nuclei size from both melanoma and normal looking, tissues were examined histologically. Skin tissue adjacent to melanoma was evaluated histologically. The following steps were sequentially performed: Materials were fixed with 10% formalin, embedded in paraffin, cut into 5 μm slices, and stained with Hematoxylin&Eosin.

Nuclei sizes were determined, taking 50 measurements from each section by using an image analysis workstation composed of the following: a personal computer running Microsoft Windows 98 operating system, a light microscope (Leica DMLB, Germany), a frame grabber card (Matrox Meteor, Matrox Inc., Canada), a digital camera attached to the microscope (Sony XC003P 3 CCD, Sony Inc, Japan), and a image analysis software (SAMBA 2000). Melanomas and non-cancerous tissues from five mice were examined. Average nuclei area from each mouse was used for statistical analysis. Differences in nuclei sizes were determined using Student's t-test.

Results and Discussion

These experiments revealed that ELSSS system can clearly differentiate between melanoma and non-cancerous skin tissues of mice. Before obtaining spectra from normal and melanoma mouse skin tissues, background spectrum $R(\lambda)_c$ and spectrum from spectralon $R(\lambda)_{bg}$ were measured to eliminate contributions of back reflected light from system components and to eliminate spectral distribution of the light source. Then, spectra from cancer-free tissue, cancer tissue (melanoma), as well as normal looking skin tissue adjacent to melanoma, were investigated. Corrected spectra have been calculated using Eq. [1] in real-time. All spectra in the wavelength range of 450-750 nm were normalized to eliminate variations in intensity. As shown in Figure 2, the spectrum slope of non-cancerous skin tissue is positive whereas the melanoma slope is negative. In Figure 2, hemoglobin absorption bands between wavelengths range of 520-590 nm do not appear on either spectrum, due to the short path length of the singly-scattered photons in tissues. In the wavelength range of visible light, absorption of melanoma displays exponential decay as a function of wavelength (16). Intensity of diffuse back-reflected light from human malignant melanoma has been shown to increase with increasing wavelength (16). In the spectrum of diffuse back-reflected light from mouse melanoma, intensity of light increased with increasing wavelength; however, intensity of singly-scattered light from mouse melanoma skin decreased with increasing wavelength. Since optical path length of singly-scattered photons is shorter than diffused photons in tissue, negative slopes of spectra in Figure 2 could not be originated from the absorption of melanoma. Other reasons, such as increased nuclei concentration within melanoma tissue, may affect spectral slope. In this study, we hypothesized that the system differentiates cancerous from non-cancerous tissues due to differences in nuclei size. Therefore, we investigated correlations between spectral slopes and nuclei sizes.

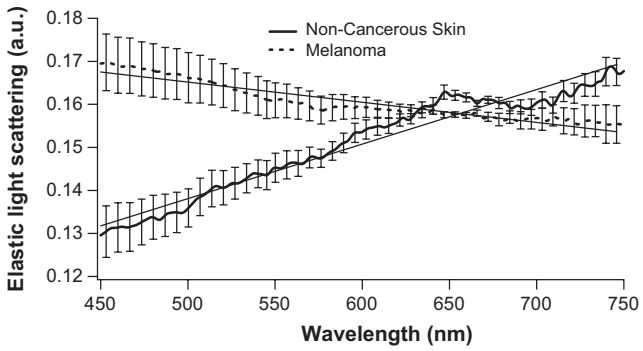


Figure 2: Slope of the spectrum of non-cancerous tissue and melanoma. Each spectrum represents averages of more than 15 spectra. Slope was negative for melanoma ($R^2 = 0.89$), whereas it was positive for non-cancerous tissue ($R^2 = 0.95$).

As shown in Figures 3a and 3b, melanoma nuclei are larger, irregular and ratios of nuclei to cytoplasm exceed those in surrounding non-cancerous skin tissue, supporting our hypothesis. Nuclear size was measured as described above. Nuclear size of melanoma was twice that of non-cancerous tissue (Figure 3c). Figure 3d shows the correlation between average nuclei area and slopes. A clear correlation occurred

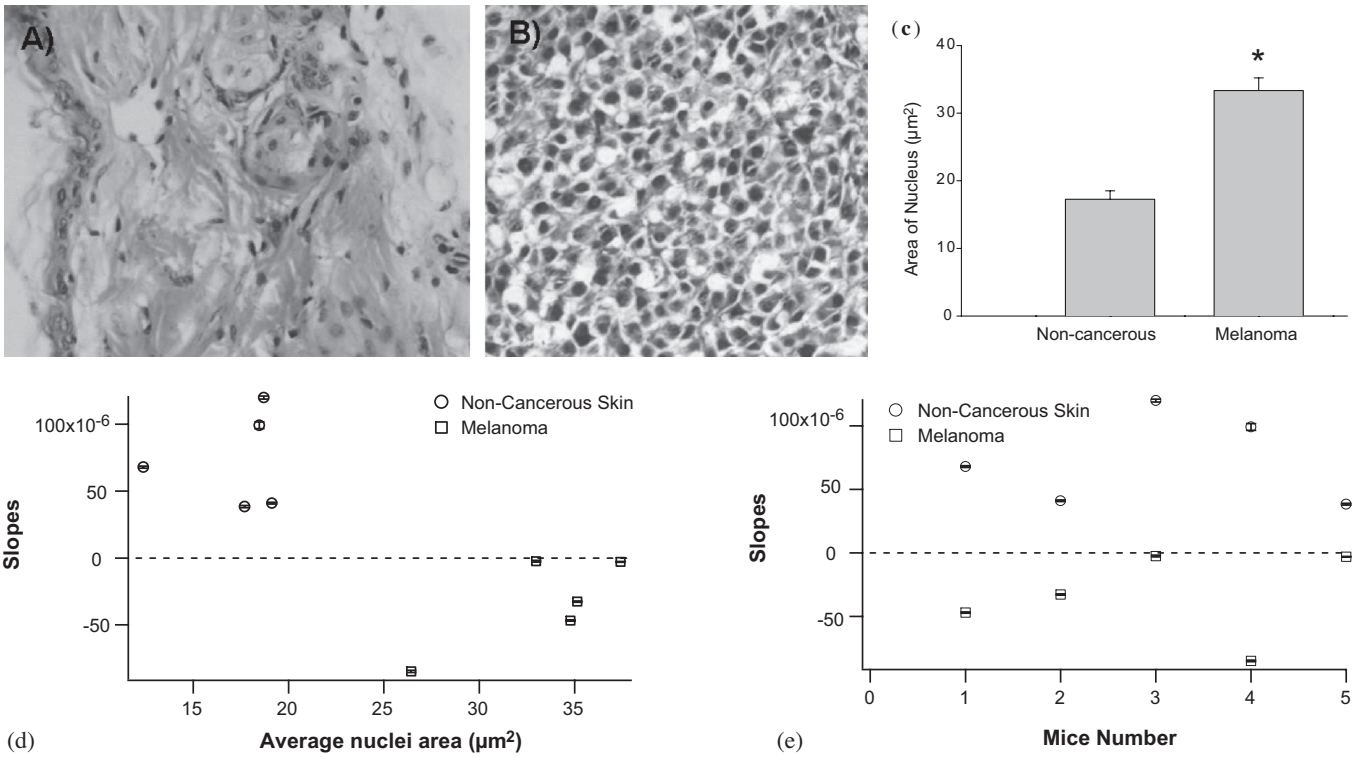


Figure 3: (**a**) Histological appearance of epidermis and dermis. There was no evidence of cancer cells, H&E X 200. (**b**) H&E staining of melanoma tissue reveals eosinophilic cytoplasm, hyperchromatic nuclei with prominent eosinophilic nucleoli. (**c**) Average area of nuclei of cancerous and non-cancerous cells. Area of nuclei was determined by using software SAMBA 2000 as described in methods, * p< 0,05. (**d**) Slopes of spectra versus nuclear size. As shown in Panel (**d**), all noncancerous nuclei were less than 20 mm^2 and slopes of the spectra were positive whereas all nuclei of melanoma tissue exceeded 25 mm^2 and spectral slopes were negative (n=5). (**e**) Correlations between histopathology results and signs of slopes.

between sizes of nuclei and spectral slopes. When nuclear size increased, slope sign became negative. We also compared slope sign with histopathological results. Figure 3e demonstrates the values of slopes of cancerous and non-cancerous tissue determined by histological examinations of each mouse. Signs of slopes for all melanoma samples were negative, whereas they were positive for non-cancerous tissue. Averages of spectral slopes taken from non-cancerous and melanoma skin tissues for those five mice were $7.33 \times 10^{-5} \pm 3.6 \times 10^{-5}$ and $-3.40 \times 10^{-5} \pm 3.43 \times 10^{-5}$, respectively.

No analytical model has yet been reported to explain marked differences in spectral slopes of normal versus cancerous tissues. However, notable similarities exist between our experimental results and the computational model of light scattering in normal and pre-cancerous cervical cells reported elsewhere. In one such study (17), Drezek *et al*. used a simulations model based on a heterogeneous population of cells, including both normal and pre-cancerous cervical cells. Light scattering from cells was calculated by a pulsed finite-difference time-domain method. In the simulation, broadband light in the range of 600-1000 nm was used. Intensity of the scattered light was integrated as a function of wavelength for different scattering angular ranges. The contrast between integrated intensities of normal and pre-cancerous cells was most apparent for the angular range of 160 to180 degrees. Intensity of scattered light increased with wavelength for normal cells, but did not change for dysplasia. Notable similarity occurred between the ELSSS spectra of our *ex vivo* experiments and spectra calculated by this simulation. Our experimental results showed that back-scattered light intensity increased with wavelength for normal cells. This resembles observations in Drezek's simulation. These simulations are consistent with our own experimental results, shown in Figure 2, where the slope for the measured spectra of normal epithelial tissue is positive, whereas the slope of spectra measured on tumors is negative. Since the numerical aperature of the optical fibers used in our probe is 0.22, the half-acceptance angle of the light is 13 degrees. The back-reflected light in the angular range of 167 to 180 degrees collected by the single optical fiber probe in our light collection geometry is similar to the geometry described in Drezek's study.

Intensity of light collected by the single-fiber optical probe is defined by size distribution of the scatterers, relative index of refraction of scatterers to surrounding medium, wavelength of light and, numerical aperature of the single-fiber optical probe. Intensity of light detected by the single- fiber optical probe as a function of wavelength is:

$$I(\lambda) = 2(\pi/k^2)\int_{167}^{180}(|S_1(\vartheta)|^2 + |S_2(\vartheta)|^2)\sin\vartheta d\vartheta. \qquad [2]$$

Where k is wave number of light, ϑ is the angle and S_1, S_2 are scattering amplitudes in Mie theory (18). As seen in Eq. [2], intensity of detected light is proportional to integration of scattering amplitude in angular range of the acceptance angle of the single-fiber optical probe. Therefore, spectral distribution of back-reflected light is defined not only by the tissue, but also by the numerical aperature and diameter of the single-fiber optical probe. This information required to calculate intensity of light with Eq. [2]. Calculating intensity of singly-scattered photons as a function of wavelength using Eq. [2] requires knowledge of the size distribution of scatters of normal and cancerous tissues.

We also observed that highly necrotic areas of tumor tissue yielded a different pattern of spectrum in all samples. Figure 4a demonstrates the histological appearance of the necrotic areas where spectra were taken. There were no visible intact cells with nuclei in necrotic tissue. This area, localized in the middle of the large mass of tumor, was probably ischemic for a long time. As seen in Figure 4b, spectra taken on necrotic tissues differed from spectra of both normal and melanoma tissues. First, intensity of the single scattered light beams decreased in wavelength range of 450 nm-580 nm, reached a minimum, and then increased within the rest of the wavelength range. This same characteristic occurred in spectra from necrotic tissues of five mice.

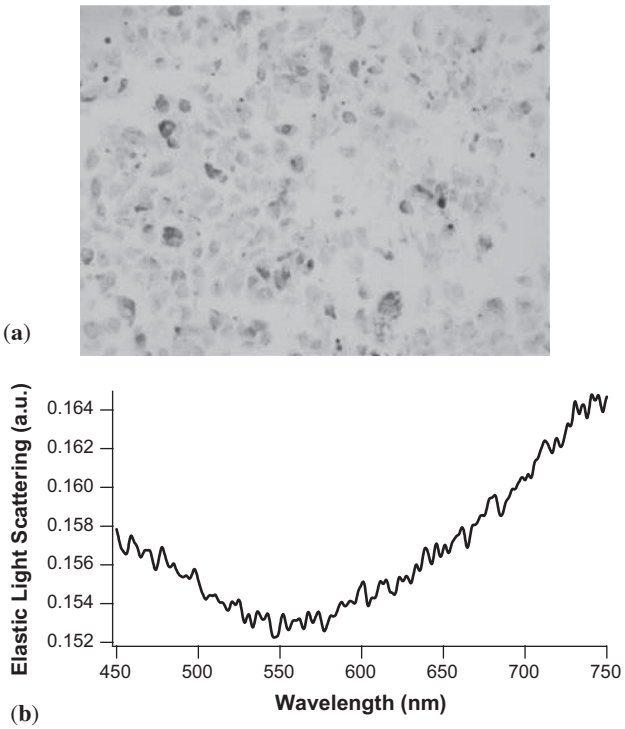


Figure 4: (**a**) H & E staining of necrotic area in melanoma (× 400). (**b**) Spectrum of necrotic tissue. Spectrum of necrotic area differed between both non-cancerous and cancerous tissues such that it first yielded a negative, then a positive, slope of spectrum (U-shaped). This was observed in all measurements taken from five different mice. From each animal, 15 measurements were taken.

We did not observe Mie oscillations in spectra from tissues. Light scatters in tissue due to variations of refraction index. Therefore, light scattering occurs in tissue when it crosses the interface of two biologic materials with different indices of refraction. In tissue, light scatters on cell membranes, on nuclei and on other cellular organelles. Sizes of scatters have broad ranges of distribution, due to variety of organelles. Therefore, overlapping of signals scattered from particles with different sizes causes disappearance of oscillations of Mie scattering.

As shown in Figure 3b, not only size of nuclei was increased, but also nuclei are closely packed in melanoma tissue. Single-scattering approximation may also be due to close packing of nuclei in melanoma tissue. Therefore, variation of spectral slopes may not only originate from enlargement of nuclei of melanoma tissue, but also by high packing of nuclei. In the current study, it has been seen that spectral slopes correlate with nuclei size. However, contribution of increased nuclei concentration to variation of spectral slopes needs to be investigated. Beside enlargement of nuclei, increased concentration of nuclei may have contributed to variation of spectral slopes. Estimating contribution of each to variation of spectral slopes needs further investigation.

Due to short optical path length of detected photons by single-fiber optical probes, contribution of tissue absorption and scattering is minimized detected signal (14). In this study, we have not specifically investigated variation of spectra acquired from different tissue types or from highly vascular tumors. For *in vivo* human experiments, caution should be employed when acquiring data from subjects with different skin colors due to variation of melanin concentration.

Only one single-fiber optical probe was used to deliver and detect light to and from tissues in this study. Since diameter of single-fiber optical probes was 100 μm, inspecting the complete surgical bed requires much time and cannot be suitable. Therefore, we currently constructed an array of the 7 × 7 single-fiber optical probe to scan 25 mm^2 tissue surfaces systematically with a resolution of 0.7 mm within a single minute. Resolution of the ELSSS system is smaller than microscopy. ELSSS system cannot replace histopathology and cannot provide detailed information concerning tissue structure. The system has potential to differentiate between cancerous and non-cancerous tissues *in vivo* and real-time. After that, pathologic examination of tissue is required for diagnoses.

The ELSSS system can be implemented to define adequate surgical margins, which may also decrease the need for on-

site histological evaluation. On-site histological evaluation may not always suffice to define surgical margins and in addition increases the time for surgery. With this system, surgical margin can be evaluated precisely since average depth of collected photons from tissue is less than 200 μm. Additionally, effects of variations of tissue absorption and scattering on spectra are negligible (10) due to short path length of collected single-scattered photons. Therefore, inter-patient variations of light scattering and absorption are unlikely. In addition, modeling of data to extract information about tissue is unnecessary, only spectral slope serves to classify cancerous and non-cancerous tissues.

Concluding Remarks

The single-fiber optical probe ELSSS system can perform "optical biopsy" to identify cancerous tissue *in situ* and in real time. This system will allow surgeons to check specimen margins during surgery to decrease the surgery time and reduce the incidence of unnecessary removal of healthy tissue. The ELSSS system cannot provide detailed information about tissue and cannot be replaced by histopathology. However, the system may differentiate normal tissue from cancerous tissue *in vivo* and in real-time. Due to short penetration depth of the collected photons, the system may not be suitable for positioning the single-fiber optical probe on skin surfaces to detect melanoma in its early stage around the basal membrane. However, the system has potential to inspect positive surgical margins of excised specimens or surgical bed. Detecting positive surgical margins may improve overall survival rate of melanoma patients after surgery.

We have conducted a pilot study with a limited number (n=5) of mice to show feasibility of ELSSS system in differentiation between melanoma and non-cancerous skin tissue. Since nearly 90% of signals collected by the single optical fiber probe originate within 200 μm depth from the tissue surface, the system is convenient to check surgical margins of excised tissues in real time without interference from underlying tissues.

Acknowledgments

This work was supported in part by EU grant MIRG-CT-2006-046565 and in part by MIRG-CT-2005-029097 and in part by Akdeniz University Scientific Research Units, Antalya Turkey.

References

1. Balch, C. M., Soong, S. J., Gershenwald, J. E., Thompson, J. F., Reintgen, D. S., Cascinelli, N., Urist, M., McMasters, K. M., Ross, M. I., Kirkwood, J. M., Atkins, M. B., Thompson, J. A., Coit, D. G., Byrd, D., Desmond, R., Zhang, Y., Liu, P. Y., Lyman, G. H., Morabito, A. Prognostic factors analysis of 17,600 melanoma patients: validation of the American Joint Committee on Cancer melanoma staging system. *J Clin Oncol 19*, 3622-3634 (2001).
2. Kaufmann, R. Surgical management of primary melanoma. *Clin Exp Dermatol 25*, 476-481 (2000).
3. Kroon, B. B., Nieweg, O. E. Management malignant melanoma. *Ann Chir Gynaecol 89*, 242-250 (2000).
4. Bishop, J. A., Corrie, P. G., Evants, J., *et al*. UK guidelines for the management of cutaneous melanoma. *Br J Plast Surg 55*, 46-54 (2002).
5. Balch, C. M., Soong, S. J., Smith, T., *et al*. Long-term results of a prospective surgical trail comparing 2 cm vs. 4 cm excision margins for 740 patients with 1-4 mm melanomas. *Ann Surg Oncol 8*, 101-108 (2001).
6. Thomas, J. M., Newton-Bishop, J., A'Hern, R., Coombes, G., *et al*. Exicion margins in high-risk malignant melanoma. *The New England Journal of Medicine 350*, 757-766 (2004).
7. Mogensen, M., Jemec, G. B. Diagnosis of melanoma skin cancer/keratinocte carcinoma: Areview of diagostic accuracy of nonmelanoma skin cancer diagnostic tests and technologis. *Dermatologic Surgery 33*, 1158-1174 (2007).
8. Mourant, J. R., Bigio, I. J., Boyer, J., Johnson, T. M., Lacey, J., Bohorfoush, A. G., Mellow, M. Elastic Scattering spectroscopy as a Diagnostic Tool for Differentiating Pathologies in the Gastrointestinal Tract: Preliminary Testing. *J Biomed Opt 1*, 192-199 (1996).
9. Ge, Z., Schomacker, K. T., Nishioka, N. S. Identification of Colonic Dysplasia and Neoplasia by Diffuse Reflectance Spectroscopy and Pattern Recognition Techniques. *Appl Spectroscopy 52*, 833-839 (1998).
10. Zonios, G., Perelman, L. T., Backman, V., Manoharan, R., Fitzmaurice, M., Dam, J. V., Feld, M. S. Diffuse Reflectance Spectroscopy of Human Adenomatous Colon Polyps *in vivo*. *Applied Optics 38*, 6628-6637 (1999).
11. Mehrubeoglu, M., Kehtarnavaz, N., Marquez, G., Duvic, M., Wang, L. V. Skin Lesion Classification Using Oblique-Incidence Diffuse Refractance Spectroscopic Imaging. *Applied Optics 41*, 182-192 (2002).
12. Perelman, L. T., Backman, V., Wallace, M., Zonios, G., Manoharan, R., Nusrat, A., Shields, S., Seiler, M., Lima, C., Hamano, T., Itzkan, I., Van Dam, J., Crawford, J. M., Feld, M. S. Observation of periodic Fine Structure in Reflectance from Biological Tissue: A New Technique for Measuring Nuclear size distribution. *Phys Rev Lett 80*, 627-630 (1998).
13. Backman, V., Gurjar, R., Badizadegan, K., Itzkan, I., Dasari, R. R., Perelman, L. T., Feld, M. S. Polarized Light Scattering Spectroscopy for Quantitative Measurement of Epithelial Cellular Structures *In Situ*. *IEEE J Sel Top Quantum Electron 5*, 1019-1026 (1999).
14. Canpolat, M., Mourant, J. R. Particle Size Analysis of Turbid Media with a Single Optical Fiber in Contact with the Medium to Deliver and Detect White Light. *Appl Opt 40*, 3792-3799 (2001).
15. Amelink, A., Bard, M. P. L., Burgers, S. A., Sterenborg, H. J. C. M. Single-Scattering Spectroscopy for the Endoscopic Analysis of Particle Size in Superficial Layers of Turbid Media. *Appl Opt 42*, 4095-4101 (2003)
16. Zonius, G., Dimou, A., Bassukas, I., Galaris, D., Tsolakidis A., Kaxiras E. Melanin absorption spectroscopy: new method for noninvasive skin investigation and melanoma detection. *J Biomed Opt 13*, 014017 (2008).
17. Drezek, R., Dunn, A., Richards-Kortum, R. A Pulsed Finite-Difference Time-Domain Method for Calculating Light Scattering from Biological Cells Over Broad Wavelength Ranges. *Optics Express 6*, 147-157 (2000).
18. Bohren C. F., Huffman D. R. *Absorption and Scattering of Light by Small Particles*. A Wiley & Interscience Inc., New York (1998).

Received: December 7, 2007; Revised: March 28, 2008; Accepted: April 10, 2008